Energy Conversion and Management 263 (2022) 115724

Contents lists available at ScienceDirect

Energy Conversion and Management

journal homepage: www.elsevier.com/locate/enconman

Hybrid power-heat microgrid solution using hydrogen as an energy vector for residential houses in Spain. A case study

Sergio J. Navas [a,b,*], G.M. Cabello González [a,b], F.J. Pino [b]

[a] AICIA- Thermal Engineering Group, Escuela Técnica Superior de Ingeniería, Universidad de Sevilla, Camino de los Descubrimientos s/n, 41092 Sevilla, Spain
[b] Dpto. de Ingeniería Energética, Escuela Técnica Superior de Ingeniería, Universidad de Sevilla, Camino de los Descubrimientos s/n, 41092 Sevilla, Spain

ARTICLE INFO

Keywords:
Smart grid
Energy management
Energy storage
Modelling
Simulation
Green hydrogen
Economic assessment

ABSTRACT

In order to favor a transition to a renewable energy economy, it is necessary to study the possible permeation of renewable energy sources not only in the electric grid or industrial scale, but also in the small householding scale. One of the most interesting technologies available for this purpose is solar energy, since it is a mature technology that can be easily installed in every rooftop. Thus, a techno-economic assessment was carried out to evaluate the installation of a solar-based power-heat hybrid microgrid considering the use of hydrogen as an energy vector in a typical residential house in Spain. Lead-acid batteries plus the photovoltaic and solar thermal energy installation are complemented with a hydrogen system composed of an electrolyzer, two metal hydride bottles, and a fuel cell. A simulation tool has been generated using experimental models developed and validated with real equipment for each one of the electric microgrid component. Three operating modes were tested making use of this tool to better manage the energy consumed/produced and optimize the economic output of the facility. The results show that setting up a hydrogen-based microgrid in a residential house is unviable today, mainly due to the high cost of hydrogen generation and consumption equipment. If only solar energy is considered, the microgrid inversion (12.500 €) is recovered in ten years. On the other hand, selling the electricity output has almost no repercussions considering current electrical rates in Spain. Finally, while using an optimization algorithm to manage energy use, battery life-spam, and economic benefit slightly increase. However, this profit may not be enough to justify the use of a more complex control system. The results of this research will help users, renewable energy companies, investigators, and policymakers to better understand the different factors influencing the spread of renewable smart grids in households and propose solutions to address these.

1. Introduction

The continuous rise in the electric bill along with the new energy transition policies towards renewable energies and the necessity of secure energy supply and reduce the energy dependence from external provenance have encouraged the use of renewable sources to cope not only with the electric, but also with the heat demand. Nowadays, more than 10% of the world's population has no access to electricity, most of them in distant rural areas. The integration of renewable energy sources and storage systems into standalone microgrids is an environmentally friendly opportunity to provide electricity and thermal energy to remote isolated areas. In this sense, many countries are studding in a depth way the deployment of microgrid as an energy efficient and reliable power system for island communities [1,2]. Furthermore, in electrified areas, the inclusion and diversification of new local renewable energy sources contribute to a reduction in greenhouse gas emissions and a decrease in energy dependence.

In developed countries, residential buildings account for approximately 30% of the energy demand [3]. This fact, together with the large amount of roof surface available (PV rooftop systems could cover up to 24% of the European electricity consumption) [4–7], makes this sector a key player when it comes to achieving greater penetration of renewable energy in the energy mix. In the industry, combined heat and power (CHP) microgrids have been shown to be successful in recovering wasted heat, increasing efficiency, and reducing pollutant gas emissions [8,9], but there are few studies that asses this issue for small household scale, and less that do it using only renewable energy. Some studies that evaluate the suitability of using a CHP microgrid for household or small rural applications contemplate the use of non-renewable energies such as diesel fuel or natural gas [10–13]. They concluded that hybridizing this kind of systems successfully cope with the household energy

* Corresponding author.
E-mail addresses: sergionavas@aicia.es, snavas1@us.es (S.J. Navas).

https://doi.org/10.1016/j.enconman.2022.115724
Received 7 March 2022; Received in revised form 21 April 2022; Accepted 4 May 2022
Available online 12 May 2022

Nomenclature

α	Power temperature coefficient
η_{MPPT}	Maximum power point tracker efficiency
$(\tau\alpha)$	Transmittance-absorptance product
θ_D	Angle of incidence direct solar radiation
θ_d	Angle of incidence diffuse solar radiation
A	Collector area
A_i	External area of inlet pipes
An	External area of zone "n"
A_o	External area of outlet pipes
A_{ST}	Heat exchange area of the storage tank
C $(\tau\alpha)$	Heat loss correction factor
C_A	Number of collectors in series correction factor
Ci	Capacitor of "i" element of the equivalent circuit
C_M	Flow correction factor
C_p	Specific heat
C_x	Energy cost of the "x" element
C_{UL}	Heat loss correction factor
CAN	Controlled Area Network
CF	Number of cycles to failure
CPH	Combined heat and power
F_{PV}	Derating factor
F_R	Heat removal factor
G	Specific mass flow
G_t	PV Incident solar radiation
G_{tSTC}	PV Incident solar radiation under standar operating condition
GC_{pi}	Specific heat capacity for the mass flow of the installation
GC_{pe}	Specific heat capacity for the mass flow of the test
i	Current
I	Solar radiation
I_d	Diffuse solar radiation
Inv	Investment cost of the batteries
I_D	Direct solar radiation
k	Thermal conductivity
K_m	Temperature correction factor
mi_{nx}	Inlet mass flow from zone "n" to zone "x"
mn	Total mass of zone "n"
mo_{nx}	Outlet mass flow from zone "n" to zone "x"
M	Mass flow through the pipes
n	Number of pannels
OPC	Ole Process Control
P_x	Power produced/consumed by "x"
PLC	Programmable Logic Controller
PV	Photovoltaic field
PVT	Photovoltaic + thermal field
Q	Hydrogen flow rate
Q_u	Useful energy
Ri	Resistance of "i" element of the equivalent circuit
SOC	State of Charge
t	Time
T_{amb}	Ambient temperature
$T_{C,STC}$	Temperature of the cell at standard operating condition
T_{fe}	Fluid inlet temperature
T_{fs}	Fluid outlet temperature
Ty	Temperature of zone "y"
T_{ONC}	Temperature of the cell at nominal operating condition
T_s	Sample time
U	Thermal transmittance
U_L	Global loss coefficient
U_t	Overall heat transfer coefficient
Vi	Voltage of "i" element of the equivalent circuit
Voc	Open Circuit Voltage
xy	Height of zone "y"
Y_{PV}	Power under standar operating condition
Zy	Zone "y" of the storage tank

demand contributing to the penetration of renewable energy and reducing dependence from the main grid, reducing energy waste and enabling the share of solar PV to be expanded without the use of large storage systems. Nevertheless, the goal of this study is to go a step further and consider only renewable options, using technologies that are well established in the market in order to cope with electricity and domestic hot water demand in an urban household. Because of that, a combination of photovoltaic and thermal solar energy has been chosen for this study, as among all the possible renewable technologies that can be used to cope with thermal and electrical supply based on renewable energy, solar technologies are the most mature, existing solutions in the market with increasingly competitive prizes. Also, studies have shown that inclusion in the grid of other renewable systems such as wind turbines [14] and biomass [15] is not as cost-effective as solutions that include only solar systems and batteries. As an example, Murty and Kumar [16] found that, for a standalone microgrid in India, the most economical configuration was a PV + battery system. On the other hand, Mohammadi et al. [17] used HOMER software and an hourly and average monthly load to investigate the best combination of PV + wind turbines + battery units for meeting the 95–100% of the demand. They found that the ratio of power generation to the investment cost of PV is better when compared to wind turbines, so it is better to always use photovoltaics instead of wind turbines even when it requires expensive systems like battery banks. Also, Pradhan et al. [15] study concludes that although biomass systems are suitable for remote off grid households, their operating cost and maintenance make them unviable from an economic point of view when compared with on-grid cases.

Solar thermal installations have been proved to be an ecological promising technique to supply hot water for residential heating and other purposes [18–20]. Recently, Košican et al. [19] simulated different solar household water heating systems in Slovakia looking for the most efficient alternative from an economical, energetic and environmental point of view. In their case study, the conversion of a traditional gas boiler into a solar system installation proved to bring significant economical savings (up to 250 euro/month) with a pay-back period under 7 years with reasonable impacts on the environment. Lamnatou et al. [21] conducted a study evaluating the sustainability of this kind of systems finding that involving recycling material such as steel and copper in their construction translates into an outstanding reduction in their environmental impact.

An interesting alternative was proposed by other authors that make use of, instead two separated solar systems, one for electricity and the other one for heat, PVT collectors, which are PV cells placed on a heat exchanger, covering in one system both purposes. For example, Herrando and Markides [22] considered the use of a hybrid PVT system for domestic heat-power applications. They found that, in the UK case, the combination of a thermal solar system with a PV had a better performance than considering only the PV in terms of covering the combined household energy demand. From a sensitivity analysis, they found that high covering factors (80 to 100%) and low cooling flow rates (20 to 80 l/h) were recommended as a tradeoff that can enhance the electrical and hot water outputs, covering the 51% of the household's electrical demand and 36% of the hot water demand. The payback period of the installation was estimated to be 11 years. On the other hand, Pardo et al. [23] used TRNSYS simulations for a building (37 inhabitants) configuration in hourly steps along one year. The proposed system, located in

central Europe, needed external support from October to February to cover the demand. From March, the PVT system covers the entire hot water demand of the building and start to have more importance in the electricity one. The system was not profitable without external incentive because of the restrictions to feed heat into the district heating system, forcing the building to rely on thermal storage which implies substantial heat losses. Anyway, overall, the PVT system produced 34% of the heat and 55% of the electricity demand of the building occupying just the 50% of the roof space and proving that it is a technologically viable way with a huge potential, especially in those regions with higher solar irradiance. Those systems are interesting in the way of making a better use of the roof space, but its efficiency and commercial availability is still far from conventional solar systems. Due to the fact that they are very compact equipment, this type of combined PVT system has been evaluated even integrated into prefabricated housing units with optimal results and payback periods below 9 years [24].

The use of hydrogen storage systems through electrolyzers, hydrogen tanks, and fuel cells is a promising solution in terms of robustness, flexibility, efficiency, and energy density as an alternative to traditional storage systems. It can be used as long-term or seasonal energy storage, accumulating hydrogen when the excess of renewable energy is high, storing it in a safe way, and turning it into energy those months when there is a renewable energy shortage. However, this technology is still in early development and new studies and demonstration projects are necessary since, nowadays, it seems that its inclusion in smart grids is not yet profitable [25]. No matter what, hydrogen has been established as a viable solution for remote applications in Canada [26,27] and Australia [28,29] and governments around the world are encouraging the green hydrogen generation as the energy vector of the future. A combination of electrolizer + H_2 tanks + fuel cell along with a PV + battery system was deeply studied by Eriksson and Gray from a technical, economic, environmental, and sociopolitical point of view [30]. They concluded that hydrogen technologies had some drawback for this kind of application since an adequate energy surplus must be ready for use to run the electrolyzer, and, the fuel cell, if incorrectly sized, rely too much on generators. Besides, this yet immature technology increases the price of the project in an unprofitable way unless government funding is considered.

On a higher scale, Gercek et al. [31,32] evaluated the installation of a smart grid powered with solar photovoltaic energy and heat pumps on a 20-household residential. They found that residential homes had a self-sufficiency of 41% over the year and every household reduced their electricity bill. This reduction was directly related to the household size and human behavioral changes from one house to another.

Different operational strategies can be assessed making use of the same microgrid structure, but looking for different objectives such as simply satisfying the power-heat demand or, on the other hand, optimizing the use of energy from the performance or the economic benefit point of view. In this way, better control and operation of this kind of hybrid system involves solving a complex function of climatic conditions, power-heat demands, equipment degradation, tariff periods, and some other factors. In this case, the life of some devices is very sensitive to the way they are operated. For example, battery life-spam depends not only on the number of charge–discharge cycles, but also on the depth of the discharges, so the equipment operation management has an impact on the economy of the whole process. In this sense, several studies [33–36] have shown that a good energy management strategy is the key to the correct and optimized use of this type of systems.

This study aims to investigate the potential of using a combination of photovoltaic energy and thermal solar energy on a residential scale to contribute to the penetration of renewable energy in the edification sector in Spain. The goal of this paper is to study the technical and economic viability of covering the electricity and hot water demand of a house with three inhabitants with a renewable system, including solar energy as energy source and batteries and hydrogen technologies for energy storage. In this sense, the novelty and main contributions of this work to the research field are highlighted in the following bullet points:

- Instant power demand consideration instead of hourly energy demand. None of the studies found in the literature present a demand per second, instead they use average values in an interval between 30 min and a whole month. This small step of time considered allows us to guarantee the coverage of the instant power demand, to observe how the transient of the different equipment affects the operation of the microgrid, and to evaluate the depth of the discharge of the battery to estimate its degradation.
- The contemplation of not only the electric, but also the hot water demand. In Spain, more of the household makes use of electric, natural gas, or butane water heaters to cover their hot water needs, while, on the other hand, the heating system are usually independent elements (stoves, radiators, heat pumps, and so on). That way, hot water is mainly used in showers and not for heating the buildings. In this sense, this study aims to cope with all the electrical and thermal consumption of a living place, since most of the studies found in the literature on microgrids focus only on the electric part.
- Inclusion of hydrogen technologies on this scale. Hydrogen technologies are receiving a lot of attention lately and are presented as good candidates for seasonal energy storage as a result of the high energy density hydrogen has. Several macro projects are rising nowadays around the world, but there are few studies that consider this technology for small scale, and fewer that use it for conventional household., so more investigations in this scale and this field of application are needed.
- The use of a tool that makes use of models developed and tested in a real experimental installation. A flexible simulation tool has been developed in the framework of this study. This tool allows to observe the behavior of the installation second by second and not hourly, as is the case with most microgrid simulation tools, incorporating models that have been tested in different conditions with real commercial equipment and considering their transient response.

This work is structured as follows. First, a brief introduction sets the reader in context and clearly explains the goal and novelty of the study. Then, in Section 2, the methodology is explained, including a description of the experimental microgrid used to obtain the different models defined next. Also, the simulation system developed and the methodology used to run the simulations are described. The paper follows explaining the results obtained from the different simulation and operation modes in Section 3 to end with a last section including the main conclusions of the study.

2. Methodology

2.1. Experimental setup

The facility used for the experiments is a versatile microgrid that allows research on the integration of renewable energy with hydrogen vector under the microgrid concept (Fig. 1a) [34,37–41]. The entire system is supervised by a programmable logic controller (PLC), being Controlled Area Network (CAN), Modbus and Ole Process Control (OPC) the systems used for the communication. Finally, a control computer has been installed in order to implement advanced controllers through a Matlab-Simulink® environment.

The experimental installation (Fig. 1b) includes a photovoltaic (PV) solar field of 4 kWp; a solar thermal system composed of 2 collectors of 2.53 m^2 and a 300 l storage tank with a 2.5 kW auxiliary resistor for hot water production; a lead-acid battery stack (24 Classic EnerSol cells of 1110 Ah with a nominal voltage of 48 V) as an electric storage system; an electrolyzer of 2.6 kW with a production of 500 l/h of hydrogen at 30 bar; a Heliocentris fuel cell of 1.5 kW; and a metal hydride storage system of 14 Nm^3. Besides, to simulate the connection to the grid or an alternative power source, the facility includes a POWERBOX LBX 6 kW

a)

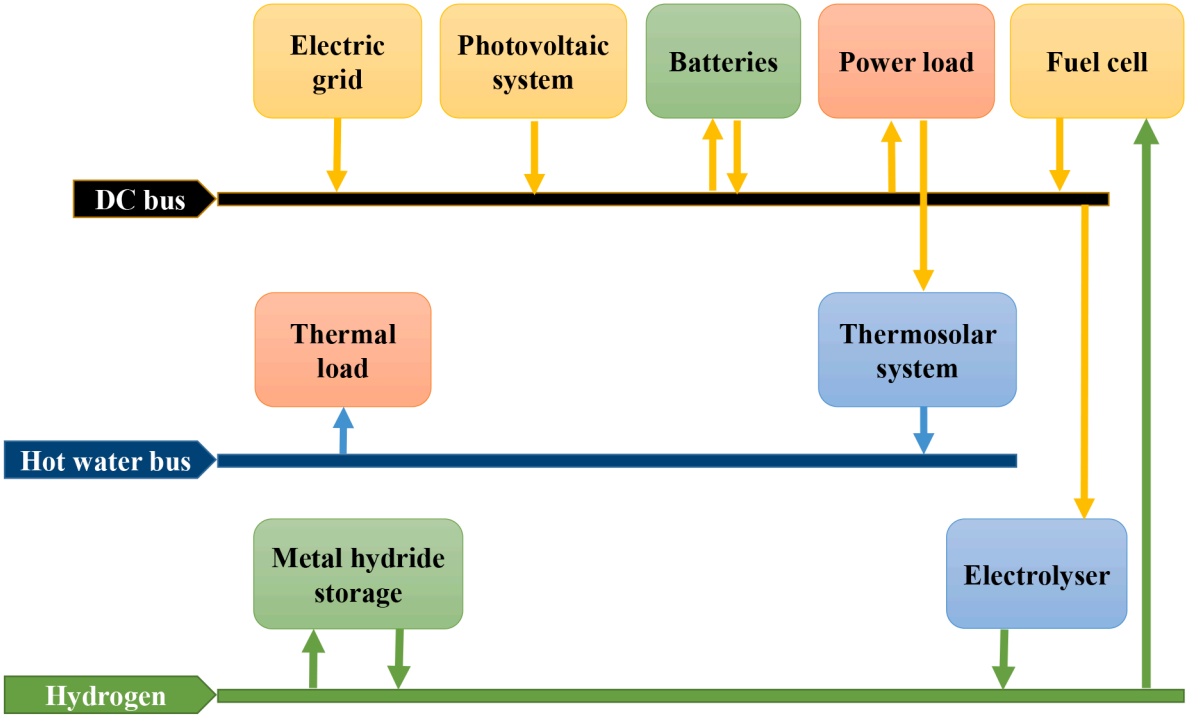

Fig. 1. Block diagram of the solar hybrid system considered (a) and micro-grid of the Thermal Engineering group (b and c).

(0–60 V / 0–100 A) electronic power source. Finally, the electric demand is simulated with an AMREL PLA 2.5 kW (0–60 V/0–1000 A) electronic load.

This same equipment will be the one included in the simulation as the different component of the microgrid proposed for the household.

2.2. Model description

This subsection describes the models of the microgrid components used in the simulations. All electric component models have been validated with real data obtained from the microgrid above described.

2.2.1. PV field

The photovoltaic field has been modelled using a static model based on parameters [42] where the power produced (P_{PV}) is given by Equation (1):

$$P_{PV} = n{\cdot}\eta_{MPPT}\left[Y_{PV}F_{PV}\frac{G_t}{G_{t,STC}}\left(1+\alpha\left(\left(T_{amb}+G_t\frac{T_{ONC}-20}{800}\right)-T_{c,STC}\right)\right)\right] \quad (1)$$

Being n the number of panels; η_{MPPT} the maximum power point tracker (MPPT) charge regulator efficiency; Y_{PV} the output power under standard operating conditions (265 kW); F_{PV} the derating factor (0.69 experimentally obtained); G_t the incident solar radiation in the photovoltaic solar array (kW/m^2) measured with the meteorological station; $G_{t,STC}$ the incident radiation under standard operating conditions (1 kW/m^2); α the power temperature coefficient (-0.0043 /°C); T_{amb} is the ambient temperature and T_{ONC} is the temperature in the nominal operating conditions of the cell (20 °C and 800 W/m^2); and $T_{C,STC}$ the temperature of the photovoltaic solar cell under standard operating conditions (25 °C).

2.2.2. Solar thermal field

The solar thermal field has been modeled with a static model based on parameters [43], where the useful energy Q_u depends on the heat removal factor (F_R), the fluid inlet temperature (T_{fe}), the global loss coefficient U_L, and the transmittance-absorptance product ($\tau\alpha$), according to equation (2), where I is the solar radiation value, A is the collector reference area, and T_{fs} and T_{amb} are the fluid outlet and ambient temperature, respectively.

$$Q_u = IAF_R(\tau\alpha) - F_RU_L\left(T_{fe}-T_{amb}\right) = MC_p\left(T_{fs}-T_{fe}\right) \quad (2)$$

The parameters $F_R(\tau\alpha)$ and F_RU_L ($F_R(\tau\alpha)$ of 0.696 and F_RU_L of 5.421 W/m^2·K) are obtained from the parameters of the yield curve provided by the manufacturer (a_{0n}, a_1 y a_2) through Equations (3) to (11), were K_m is the temperature correction factor, C_M the flow correction factor C_A the number of collectors in series correction factor and $C_{(\tau\alpha)}$ and C_{UL} the heat loss correction factor.

$$F_R(\tau\alpha) = K_mC_MC_AC_{(\tau\alpha)}a_{0n} \quad (3)$$

$$F_RU_L = K_mC_MC_AC_{UL}(a_1 + a_2{*}40) \quad (4)$$

$$K_m = \left(1-\frac{F_RU_L}{2GC_p}\right)^{-1} \quad (5)$$

$$C_M = \frac{GC_{pi}\left(1-exp\left(\frac{-F'U_L}{GC_{pi}}\right)\right)}{GC_{pe}\left(1-\exp\left(\frac{-F'U_L}{GC_{pe}}\right)\right)} \quad (6)$$

$$F'U_L = -GC_{pe}ln\left(1-\frac{F_RU_L}{GC_{pe}}\right) \quad (7)$$

$$C_A = \frac{1-(1-K)^N}{NK} \quad (8)$$

$$K = \frac{F_RU_L}{GC_{pi}} \quad (9)$$

b)

c)

Fig. 1. (*continued*).

$$C_{(\tau\alpha)} = \frac{1}{1+\frac{U_t A_o}{MC_p}} \tag{10}$$

$$C_{UL} = \frac{1-\frac{U_t A_i}{MC_p}+\frac{U_t(A_i+A_o)}{AF_R U_L}}{1+\frac{U_t A_o}{MC_p}} \tag{11}$$

being C_p the specific heat, G the specific mass flow of the installation (0.02 kg/s·m^2), GC_{pi} and GC_{pe} the specific heat capacity for the mass flow of the installation and the test, respectively, U_t the overall heat transfer coefficient of the pipes, M the mass flow through the pipes, A_i and A_o the external areas of the field inlet and outlet pipes, and A is the collector area.

Finally, it is necessary to correct the solar radiation value as a function of the angle of incidence. In this way, the irradiance is calculated following Equations (12) to (14):

$$I = K_D I_D + K_d I_d \tag{12}$$

$$K_D = 1 - b_0\left(\frac{1}{Cos(\theta_D)} - 1\right) \tag{13}$$

$$K_d = 1 - b_0\left(\frac{1}{Cos(\theta_d)} - 1\right) \tag{14}$$

where θ_D and θ_d are the angle of incidence of direct and diffuse (whose value can be assumed to be constant and equal to 60°) solar radiation respectively, b_0 is a parameter obtained from the value of K_D supplied by

the manufacturer for an angle of incidence of 50°, and I_D and I_d are direct and diffuse solar radiation respectively.

2.2.3. Hot water storage tank

The 300 l hot water storage tank (Fig. 2) was divided into 5 areas of different volumes: water inlet (Z1), heating coil (Z2), middle (Z3), electric resistor (Z4) and water outlet (Z5).

Each part is modelled according to the mass and heat balance between itself and the contiguous part. For example, the middle area was modelled using Equations (15) to (19):

- Mass balance

$$mi_{23} = mo_{23} \tag{15}$$

$$mo_{34} = mi_{23} + \partial m3/\partial t \tag{16}$$

$$mi_{43} = mo_{43} \tag{17}$$

$$mo_{32} = mi_{43} \tag{18}$$

where mi_{23} is the mass flow from Z2 to Z3, mo_{34} is the mass flow from Z3 to Z4, mi_{43} is the mass flow from Z4 to Z3, mo_{32} is the mass flow from Z3 to Z2, and m_3 is the total mass of Z3.

- Heat balance

$$m3{\cdot}c_p{\cdot}\partial T3/\partial t = mi_{23}{\cdot}c_p{\cdot}T2 + mi_{43}{\cdot}c_p{\cdot}T4 - mo_{34}{\cdot}c_p{\cdot}T3 -$$

$$- mo_{32}{\cdot}c_p{\cdot}T3 + (k{\cdot}A_{ST})/\Delta x3(T4 - T3) - (k{\cdot}A_{ST})/\Delta x3(T3 - T2) - UA3(T3 - Tamb) \tag{19}$$

where c_p is the specific heat, T is the temperature of the different zones (Z2, Z3, and Z4 in this case), k is the thermal conductivity, A_{ST} is the heat exchange area, x is the height of the corresponding zone, U is the thermal transmittance, A3 is the external area of the cylinder of Z3, and T_{amb} is the ambient temperature.

2.2.4. Electrolyzer

The electrolyzer has been modeled using real data obtained in operation within the microgrid. Equation (20) relates the flow of H_2 produced as a function of the power supplied.

$$Q = 0.2313{\cdot}P + 30.548 \tag{20}$$

where Q is the flow rate of H_2 in Nl/h and P is the power in W. Furthermore, a dead time of 60 s has been considered between when the power set point change occurs, and that value is reached.

2.2.5. Fuel cell

The fuel cell together with its associated converter has also been modeled using real data obtained in operation within the microgrid. Equation (21) relates the flow of H_2 consumed as a function of the power demanded.

$$Q = 0.0115{\cdot}P - 0.1716 \tag{21}$$

where Q is the H_2 flow rate in Nl/min and P is the power in W. For the dynamic part of the model, a first-order model with a gain of 1 and a time constant of 78 s.

2.2.6. Metal hydride storage tanks

The two metal hydride tanks for the storage of the produced H_2 have been modelled using Equation (22),

$$SOC_k = SOC_{k-1} + \left(\frac{Q{\cdot}T_s}{14000}\right){\cdot}100 \tag{22}$$

where SOC is the state of charge in %, Q is the H_2 flow rate in Nl/s, and T_s is the sample time.

2.2.7. Lead-Acid batteries

The lead-acid battery bank has been modeled after an equivalent electrical circuit (Equations (23) to (25)). This model allows knowing both the state of charge (SOC) and their voltage. The proposed equivalent electrical circuit consists of a resistance (R) in series with two other elements composed of a resistance in parallel with a capacitor (C), which results in a second-order model with two time constants. The model parameters depend on the battery SOC according to Equations (26) to (35).

$$\dot{v}_1 = -\frac{1}{R_1C_1}v_1 + \frac{1}{C_1}i_{bat} \tag{23}$$

$$\dot{v}_2 = -\frac{1}{R_2C_2}v_2 + \frac{1}{C_2}i_{bat} \tag{24}$$

$$v_{bat} = Voc - R_0i_c - v_{1c} - v_{2c} - R_0i_d - v_{1d} - v_{2d} \tag{25}$$

$$R_{0C} = 0.00000461{\cdot}SOC^2 - 0.000565{\cdot}SOC + 0.0572 \tag{26}$$

$$R_{1C} = 0.00159{\cdot}SOC + 0.0308 \tag{27}$$

$$C_{1C} = -437.8{\cdot}SOC + 52255.15 \tag{28}$$

$$R_{2C} = 0.000366{\cdot}SOC + 0.00527 \tag{29}$$

$$C_{2C} = 4000 \tag{30}$$

$$R_{0d} = 0.00000455{\cdot}SOC^2 - 0.000587{\cdot}SOC + 0.0575 \tag{31}$$

$$R_{1d} = 0.041 \tag{32}$$

$$C_{1d} = -318.99{\cdot}SOC + 58903.29 \tag{33}$$

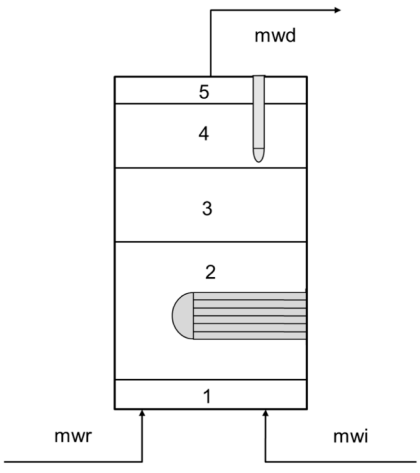

Fig. 2. Thermal storage tank schematic.

$$R_{2d} = 0.000171 \cdot SOC + 0.000858 \quad (34)$$

$$C_{2d} = 5500 \quad (35)$$

where V_{OC} is the open circuit voltage, v_1 and v_2 are the voltage values of the corresponding RC element, R_1 C_1 and R_2 C_2 are a resistor and a capacitor that describe the short- and long-term transient behaviour, respectively, and i_{bat} is the value of the current of the battery output, which is positive when discharging and negative when charging. In addition, subscripts c and d represent the charging and discharging processes, respectively.

Besides, SOC and V_{OC} correlate according to Equation (36).

$$Voc = 0.0494 \cdot SOC + 45.883 \quad (36)$$

2.2.8. Validation of the models

The models of the microgrid's electrical components have been experimentally validated using the equipment described in 2.1. As can be seen in Fig. 3, these components are the electrolyzer (top left), fuel cell (top right), PV (bottom left), and the lead acid batteries (bottom right). The fit of the model data to the experimentally measured results presents very low errors and therefore these models allow the precise simulation of the behaviour of the different equipment.

2.3. Operation modes

This section describes the operation modes evaluated in this paper. Three different modes were developed with an increasing range of complexity. The first one (OP1) was based on a self-regulatory control that makes use of lead-acid batteries as an energy buffer. The second one (OP2) bases its control strategy on a series of heuristic rules, similar to the one proposed in Valverde et al. [38] for the part-load mode. Finally, the third one (OP3) makes use of an optimal controller to operate the microgrid with the aim of minimizing the economic cost.

2.3.1. Mode OP1

The microgrid selected for Mode OP1 is composed of a PV solar field for electricity demand, a thermal solar field with a thermal storage system for hot water supply, and lead-acid batteries as an electric storage system. The operation of the microgrid in this mode is as follows: the PV system provides the electric energy consumed by the household. In case of an energy surplus, this is sent to batteries that will store the excess of electricity until 95% of the state of charge (SOC). From this SOC value, the energy generated by the PV system may be sold to the grid. When there is an energy shortage due to the lack of the required solar radiation, the energy demand will be supplied by the batteries. If, at the end of the day, the SOC of the batteries is less than 35%, they will be charged from the grid during the cheap energy period until the SOC reaches a 50% or that period ends. At the same time, the solar thermal energy system produces and stores hot water until a temperature of 85 °C in Z5 is reached in the storage tank. In case that hot water temperature is below 50 °C, we have considered that the user will start an electric 2.5 kW resistor 50 min before the shower. In this way, the facility control strategy can be easily and inexpensively implemented in a real installation.

2.3.2. Mode OP2

The microgrid chosen for mode OP2 is the same as that used for mode OP1 with the addition of an electrolyzer, a fuel cell, and a metal hydride tank storage system. In this case, the operation of the facility is regulated by a heuristic controller based on the following rules: when there is solar radiation, the PV system provides the electric energy demanded by the house. If there is an energy surplus, it is sent to the batteries first until 95% of their state of charge (SOC). From that SOC value, the electricity produced by the PV system can be used in two different ways: (i) being used to produce hydrogen with the electrolyzer if the PV production is greater than 1.1 kW (the minimum operation point of the electrolyzer) and the SOC of metal hydrides storage tanks is less than 95%, or (ii) sold into the grid if the former requirements are not met. When solar energy is not enough to satisfy the electricity demand, it will be supplied first by batteries until they reach a 40% SOC. From that point, if the SOC of the metal hydride storage tanks is greater than 50%, the fuel cell starts producing 1 kW until a battery SOC of 50% is reached or the SOC of the metal hydrides drops to 40%. If the SOC of the batteries is under 35% when the cheap energy period starts, they will be charged from the grid until the SOC reaches 50% or that period ends. At the same time, the solar thermal energy system follows the same rules described in mode OP1.

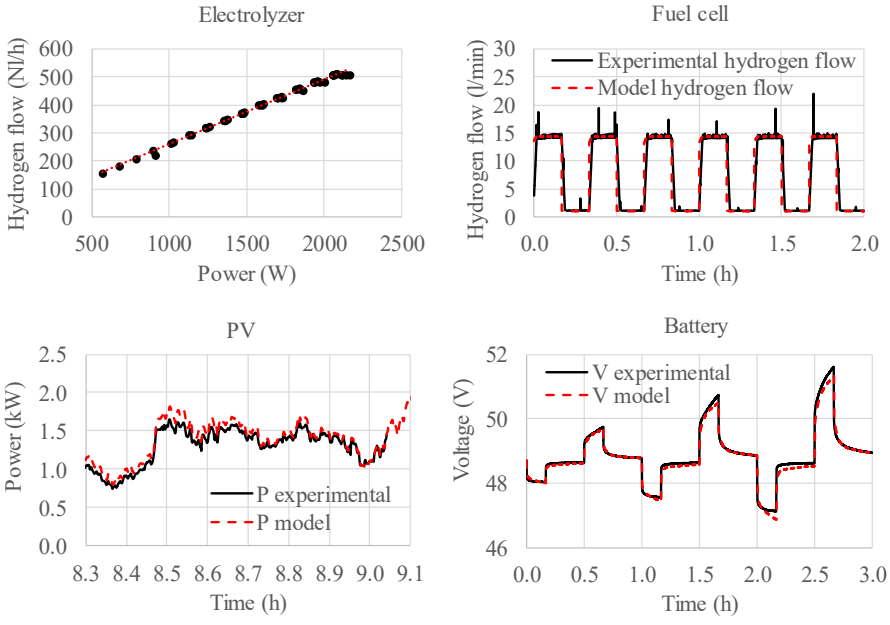

Fig. 3. Model results vs experimental data for the different models developed with the microgrid.

2.3.3. Mode OP3

The microgrid selected for Mode OP3 is the same as that used for Mode OP1. The reason why this mode does not contemplate the use of hydrogen will be discussed in Section 3. This mode of operation is the most complex of the three proposed, since it is based on the use of an optimization algorithm that minimizes a function objective. The objective function selected for this case is.

$$J = P_{grid} \cdot t \cdot C_{grid} - P_{sale} \cdot t \cdot C_{sale} - P_{bat} \cdot t \cdot C_{bat} \quad (38)$$

Subject to.

$$0 \leqslant P_{grid} \leqslant 3450W \quad (39)$$

$$0 \leq P_{sale} \leq P_{PV} \quad (40)$$

where P_{grid}, P_{sale} and P_{bat} are the values of power purchased from the grid, sold to the grid, and sent/removed from the batteries, respectively. While C_{grid}, C_{sale}, and C_{bat} are the costs of the energy purchased from the grid, sold to the grid and the use of batteries respectively. Finally, the value of t corresponds to the time in hours selected for the optimization step, in this case 10 s.

The group of constraints sets the value of the variable P_{grid} between 0 and the value of the power contracted to the grid, and the variable P_{sale} between 0 and the value of the power produced by the photovoltaic field to prevent selling the energy stored in the batteries.

The optimization algorithm selected for the simulations is the MATLAB "fmincon" function. This function will be executed every 10 s, and from the values of the input variables, which are the power produced by the photovoltaic field P_{PV} and the power demanded P_{dem}, it will determine the value of the independent variables P_{grid} and P_{sale} that minimize the objective function. In this case, the variable P_{bat} is a dependent variable, since with the configuration of the microgrid used, the batteries always absorb surpluses/deficits of energy; therefore, the value of the variable P_{bat} is.

$$P_{bat} = P_{PV} + P_{grid} - P_{dem} - P_{sale} \quad (41)$$

The purchase and sale costs used in the objective function were obtained from the prices of a Spanish electric company. On the other hand, the cost of batteries has been estimated based on their investment cost and the durability model based on the remaining discharge cycles until failure [44], so that each time the batteries are charged, the value of the objective function decreases (representing the savings that will result from storing excess energy instead of selling it) and that each time they are discharged, the value of the objective function increases (due to degradation of the battery by the discharge cycle). Likewise, a desirable operating value of 60% SOC has been set for the batteries, so that, moving away from it results in a higher cost for discharging them or less savings for charging them, in such a way as to prevent the batteries from operating at their extreme values of SOC, and thus preventing excessive degradation. The cost of the batteries is calculated using equation (42).

$$C_{bat} = \frac{\left(\frac{Inv/CF}{Ah}\right) \cdot \left(1 + \left(\lambda \cdot \left(\frac{60-SOC}{100}\right)\right)\right)}{V_{bat}} \quad (42)$$

where I_{nv} is the investment cost of the batteries, CF is the number of cycles to failure (in this case a value of 8000 cycles was selected), Ah is the value of the depth of discharge in Ampere-hour corresponding to the number of cycles to failure selected (in this case 110 Ah, that is the 10% of the batteries capacity), V_{bat} is the batteries voltage, and λ is a weight factor that penalizes the use of the batteries while the SOC is far away from the reference value of 60%. This factor may have different values for the charge and discharge processes.

2.4. Simulation system

Simulations of the operating modes have been carried out with the Matlab-Simulink® simulation tool. A user-friendly masked system has been developed that interconnects the different microgrid subsystems. These subsystems are composed of circuits that correlate the different variables through a Matlab function, including the mathematical equations that govern each component. That way, the simulation tool developed could be easily changed to evaluate different microgrid configurations.

The electricity demand consists of real data measured from a residential home for a whole week [45], in the form of power measurements per second. The hot water demand has been considered to be due to 3 showers of 5 min with a flow rate of 20 l/min and a temperature of 38 °C (this temperature is obtained by mixing the hot water with the cold water, which requires hot water to be at a temperature greater than or equal to 50 °C to guarantee that the mixing temperature of 38 °C can be reached at all times) carried out at different times of the day (7:00, 18:30, and 21:00). Climate data were those of a typical meteorological year (Meteonorm® software) in the province of Seville.

The same procedure has been followed for the simulation of the three modes. A week has been selected for each month of the year, starting with the month of July, assuming that this month begins with the maximum values of SOC (which is verified to be a correct assumption after simulating the entire year) of the different storage systems corresponding to the simulated mode (batteries for all of them and metal hydrides only for mode OP2). The first step is to simulate the selected week of the corresponding month. If after the simulation of the week, the SOC values remain stable (with a difference of +/- 4%), it is assumed that the behavior of the month will be the same as that of the simulated week, and therefore the energy calculations bought/sold to the grid would be the result of multiplying by 4 those obtained with the simulation of that week. However, if the state of charge values varies from starting ones after the week's simulation, simulations continue for that week until either the states of charge stabilize or 4 simulations have been performed for that month (see Fig. 4). This process is repeated for each month until a year is completed. Once the year has been simulated, the total energy purchased from the grid, as well as the energy sold to the grid, can be calculated. With these data, an economic study is carried out that allows determining when the return on investment occurs for each of the proposed modes of operation, using the electric bill data of a house without a microgrid as the base case.

2.5. Economic evaluation

A tariff from a Spanish electricity distribution company has been chosen for the grid connected base case, considering three periods during the day: peak (0.24442 €/kWh), shoulder (0.15097 €/kWh), and valley (0.11644 €/kWh), and a contracted power of 5.75 kW, as 5 kW is the highest peak observed in the house demand profiles. On the other hand, for the first, second, and third case study, a lower power contracted is necessary because the main peaks of demand are met with the solar energy and the batteries, not with the grid, so a contracted power of 3.45 kW was considered. In this case, a defined for solar energy users' tariff was chosen because it allows to sell energy into the grid. This tariff considers a regular (0.242028 €/kWh) and a cheap period (0.194955 €/kWh) and buy the output energy (0.051 €/kWh). Moreover, in Spain, there is a specific tax on electricity of 0.5% and a VAT of 10% that affects the entire bill.

The inversion and installation cost of buying and installing the different equipment in the house has been considered as follows: electrolyzer 38,000 €, metal hydrides 16,000 €, fuel cell 11,200 €, lead-acid batteries 5500 €, photovoltaic solar field 5000 € and thermal solar field 2000 €. That way, the initial inversion for the first and the third case study rises to 12,500 €, while in the second case the necessary amount of money is 77,700 €.

In this study, the fact that the electrolyzer and fuel cell should be replaced after a 10-year and 12-year period respectively with a cost of 50% over the initial investment, and the PV, solar thermal system and

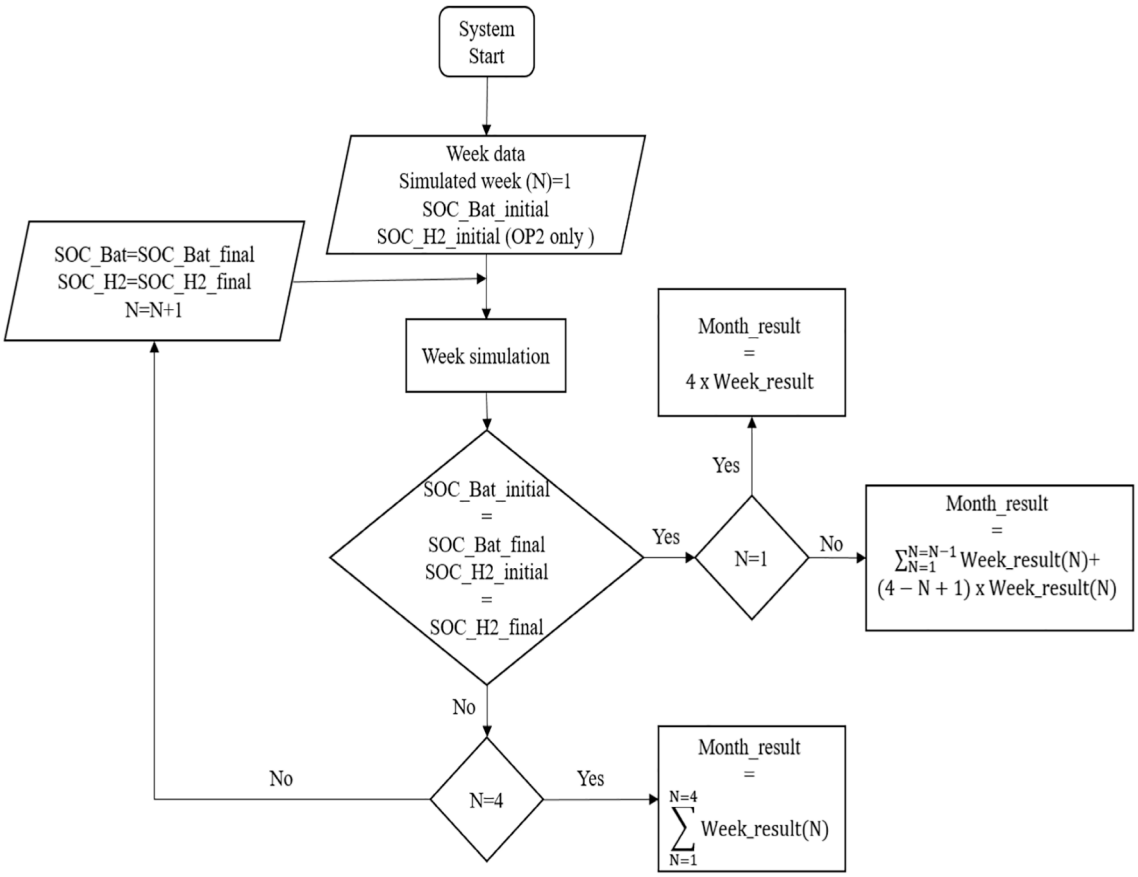

Fig. 4. Algorithm for the simulation of the operation modes.

metal hydrides after a 25-year period with full cost was considered. Therefore, the economic evaluation will be done for a 25-year period in order to consider all the component replacements. Battery replacement has also been considered, but in this case, instead of having a fixed replacement period, such as solar installations, its durability has been estimated using a degradation model [44] that takes into account the number of cycles and the depth of the discharge of batteries. These costs include maintenance and possible part substitution. This will be a worst-

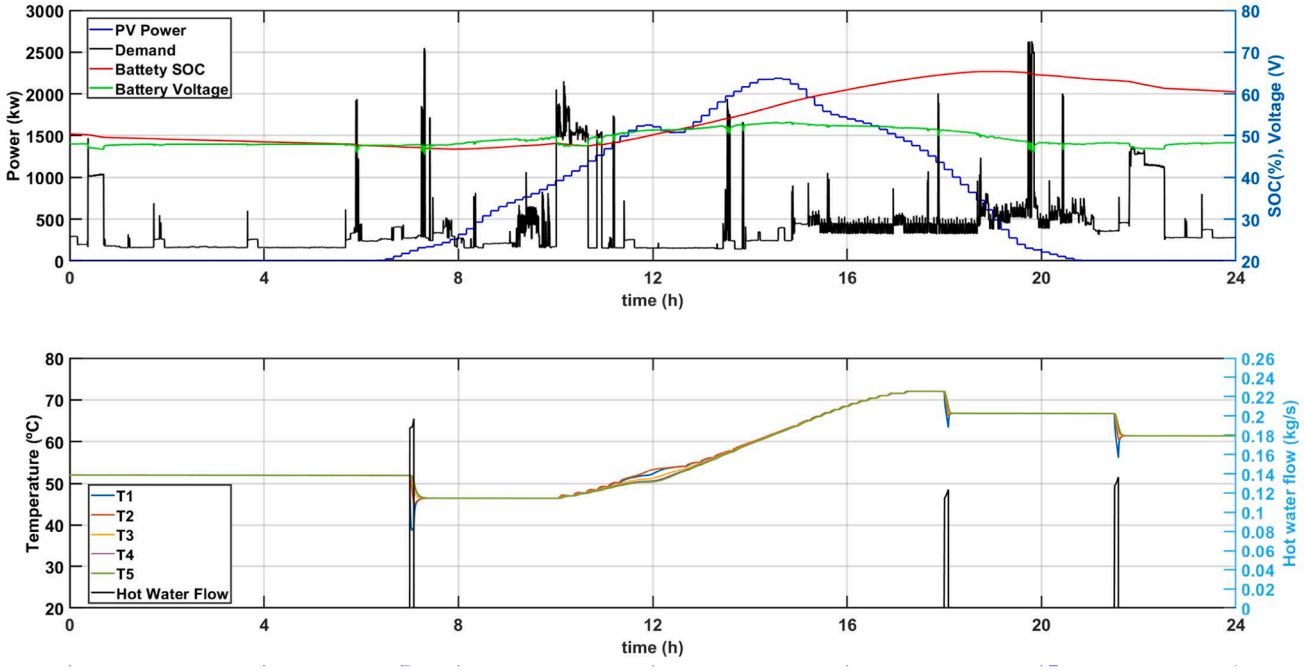

Fig. 5. Simulation result for a June day in Mode OP1 (June 9).

case scenario, because the development of these technologies will make equipment substitution more affordable economically.

3. Results and discussion

This section describes and analyzes the results obtained during the simulation process of the operation modes proposed in this paper for the energy management of the microgrid. It also contains the authors' discussion about the results presented and the comparison between them, highlighting the advantages and disadvantages of each operating mode. Finally, the section concludes with the reasons why the authors think which operation mode is suited for the case study.

The three operation modes shown in Section 2.3 were simulated following the procedure described in Section 2.4. The results obtained with these simulations were then assessed against a base case study. This base case considers a traditional three-inhabitant household fully dependent on the electric grid. The total amount of energy consumed by the house yearly is: 1992 kWh peak period, 2076 kWh shoulder period, and 960 kWh valley period, which makes a 1321 €/year energy bill in the base case.

The simulation of the Mode OP1 considers the same household where a microgrid composed of a PV solar field for electricity demand, a thermal solar field with a thermal storage system for hot water supply, and lead-acid batteries as an electric storage system, is installed. An example of a one-day simulation of a sunny summer day can be seen in Fig. 5. The upper part shows the power demand, the PV generated power, the battery voltage, and the battery SOC; the lower part shows the temperature distribution inside the storage tank of the solar thermal energy system and the hot water demand. Since it is a high irradiance day, the PV system can deal with the energy demand, except at the beginning and the end of the day. There is also an excess of energy during the middle of the day that is stored in the batteries, so their SOC, at the end of the day, is higher. Also, the solar thermal field can supply the hot water demanded for every shower and increase the tank temperature due to the energy excess. Fig. 6 shows the simulation for a whole week in June, where, since it is a summer month with high irradiance values, solar energy covers all the electricity demand (black line), the batteries are kept at about reasonable voltage levels (green line) always being around 90% of SOC (red line) and almost a third of the energy produced during the day (blue line) can be sold to the grid (break in the blue line). In this scenario, the PV coupled with batteries can supply the daily power demand, except between the months of November to March, where some of the days, batteries must be charged during the night to ensure the next day's power demand. These transitional months in terms of energy were also observed by Pardo et al. [23] using a PVT system in Central Europe. The total amount of energy extracted from the grid annually is 328 kWh (Table 1). That way, the annual power bill rises to 315 €/year, four times less than in the base case. Besides, from May to October, a total of 782 kWh can be sold to the grid, generating around 40 €/year.

Figure 7 shows the cumulative cash flow obtained with mode OP1 for every year of the 25 year period considered. It can be seen that the amortization of the facility occurs in 10 years considering that the surplus energy is sold, and in 11 years if it is not. This same payback period was estimated by Herrando and Markides [22] after the optimization of a PVT system, but without electric energy storage systems, which still makes these combined systems a bit less profitable than the separated PV + thermal solar energy ones. An initial investment of 12,500 € with an amortization period of 10 years may seem a bit tight for the average Spanish family. According to the INE, the savings rate for Spanish families is 6.1%, which means that for every 1000 € earned, 61 € are saved; and the average monthly savings amounts to about 300 €. Nevertheless, with the ever-increasing electricity price, it is likely that this period will be significantly reduced in the short term. On the other hand, selling energy slightly benefits the economics of the facility, reducing the amortization period in one year and increasing the benefit in around 1900 € at the end of the period. Still, the difference between the purchase price of electricity (around 0.19 €/kWh) and the price at which a household can sell its excess of renewable energy (0.051 €/kWh) significantly limits the acquisition of this type of system by private users.

The option of being isolated from the grid was also assessed, but it

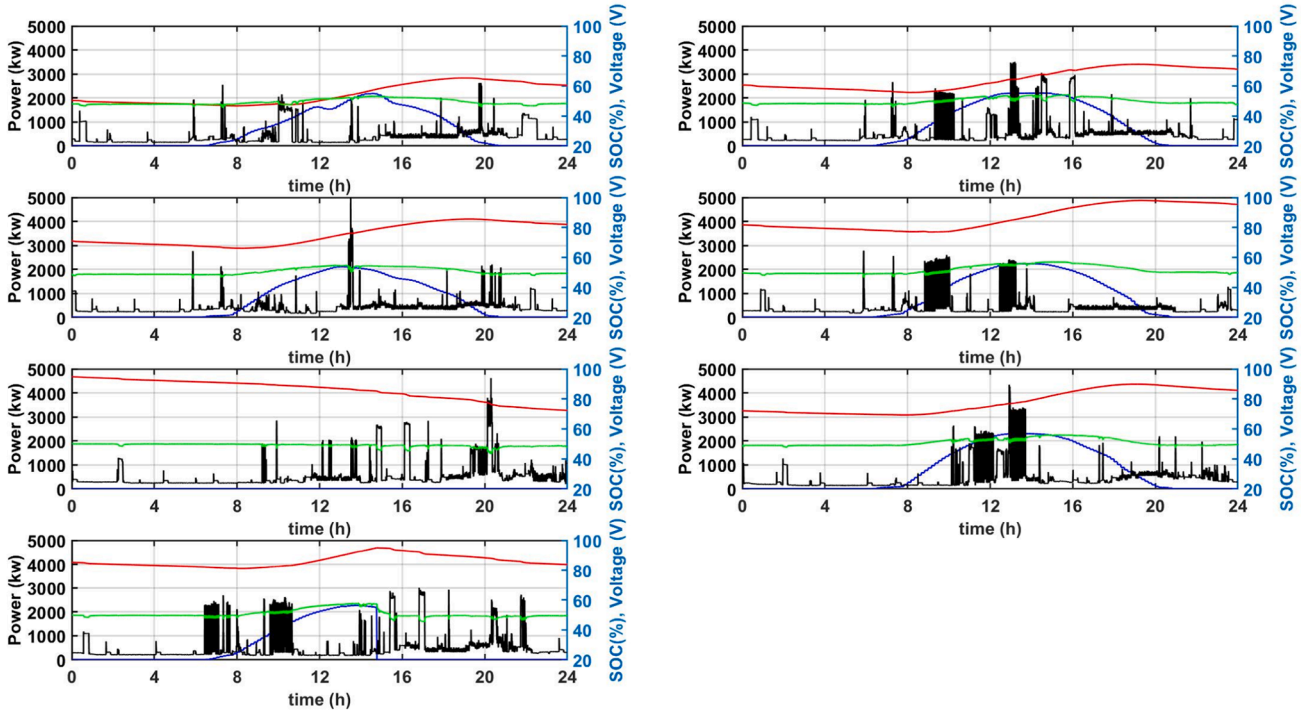

Fig. 6. Simulation of a week in June using Mode OP1. Demand profiles (black), power generated by the photovoltaic field (blue), voltage (green), and state of charge (red) of the batteries.

Table 1
Energy consumed from and sold to the grid.

	OP1		OP2		OP3	
	Energy consumed	Energy sold	Energy consumed	Energy sold	Energy consumed	Energy sold
JANUARY	78.58	0.00	78.58	0.00	95.53	0.00
FEBRUARY	79.24	0.00	79.24	0.00	67.10	0.00
MARCH	116.81	0.00	116.81	0.00	101.56	0.00
APRIL	0.00	19.92	0.00	0.00	0.00	32.84
MAY	0.00	156.03	0.00	139.62	0.00	162.32
JUNE	0.00	169.00	0.00	169.00	0.00	178.29
JULY	0.00	173.00	0.00	173.00	0.00	191.60
AUGUST	0.00	99.40	0.00	99.40	0.00	122.36
SEPTEMBER	0.00	93.20	0.00	93.20	0.00	97.34
OCTOBER	0.00	68.16	0.00	68.16	0.00	68.76
NOVEMBER	2.84	3.34	0.00	3.34	11.87	6.99
DECEMBER	50.50	0.00	43.65	0.00	45.32	0.00
TOTAL (kWh)	**327.97**	**782.05**	**318.28**	**745.72**	**321.38**	**860.50**

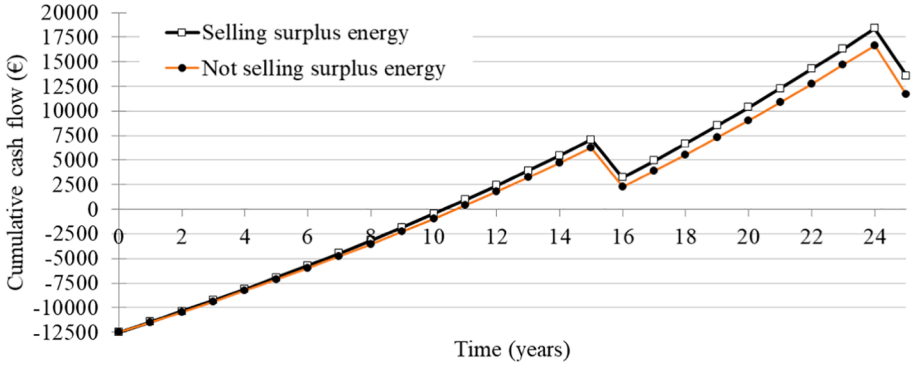

Fig. 7. Cumulative cash flow over a 25-year period for case one OP1 (solar energy + batteries).

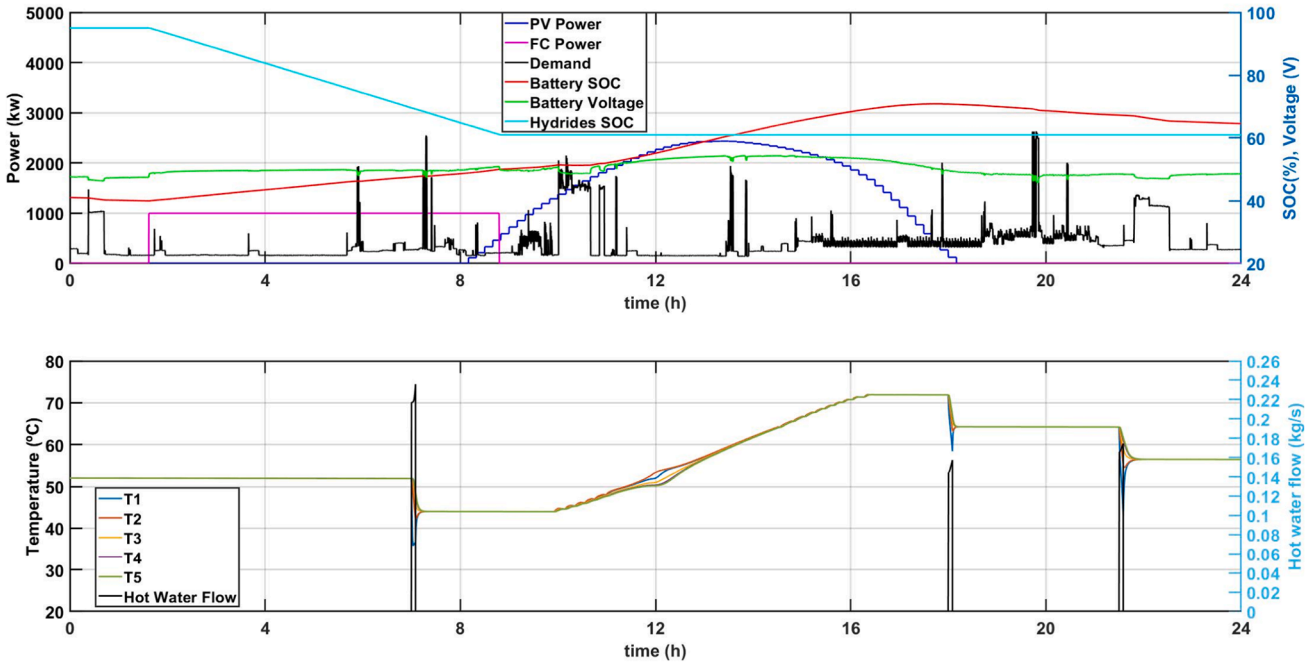

Fig. 8. Simulation result for a November day in Mode OP2 (November 2).

proved to be unfeasible. To make it viable, it would be necessary to increase the battery's capacity, so that the 328 kWh extracted from the grid could be provided by them. That amount of energy would be taken from the energy excess of 782 kWh sold to the grid. However, the investment required for such increase would lead to an economically nonviable solution, not to mention the space that would be necessary in a home to house this number of batteries in a suitable place.

For the simulation of mode OP2, whose operation is based on the application of heuristic rules that will define the behavior of the microgrid, a green hydrogen system was considered in addition to solar

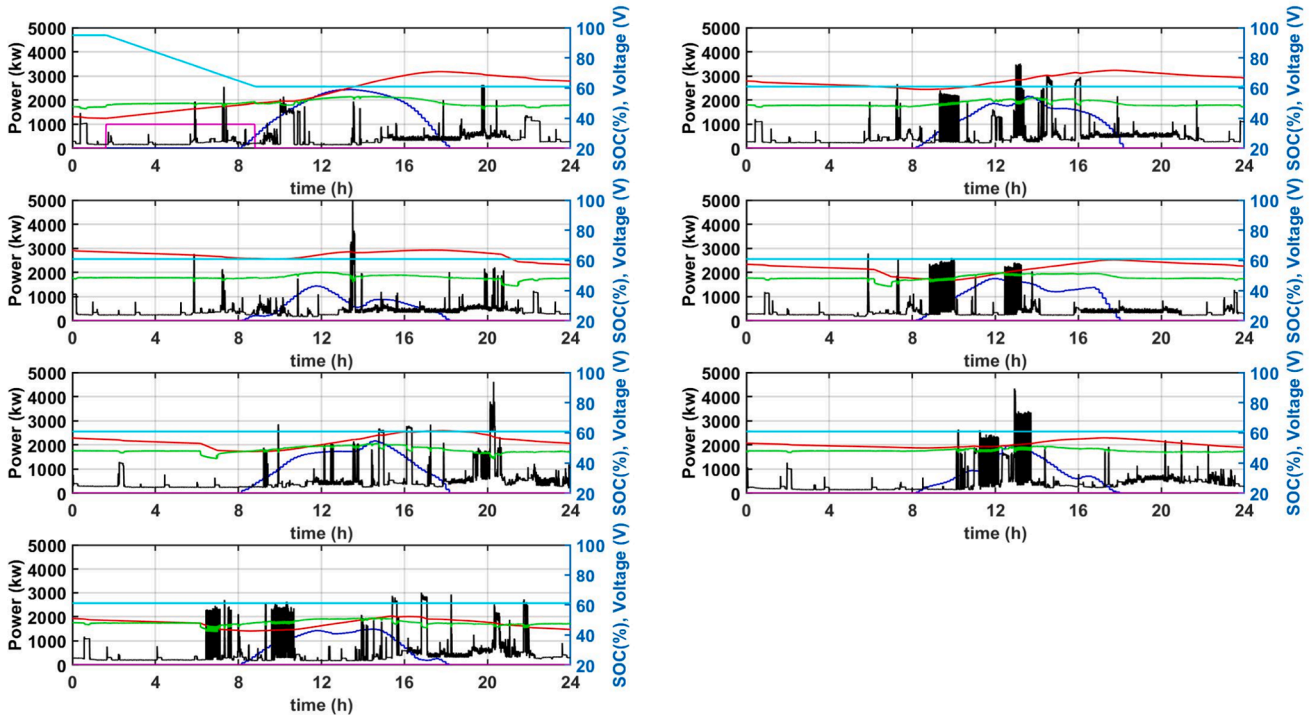

Fig. 9. Simulation of a November week in the second case. Demand profiles (black), power generated by the photovoltaic field (blue), voltage (green), state of charge of the batteries (red), power generated by the fuel cell (magenta) and state of charge of the hydrides (cyan).

and battery systems. In this way, an electrolyzer, metal hydride tanks, and a fuel cell were also included. An example of a one-day simulation of November can be seen in Fig. 8, and the simulation of a November week can be seen in Fig. 9. In this case, two new variables, the fuel cell power (magenta line) and the metal hydrides SOC (cyan line), are represented in addition to the voltage and SOC of the batteries, the PV power, and the demand. Due to the lack of solar radiation during the November week represented, on the first day, the hydrogen fuel cell must intervene to meet demand reducing the hydrides SOC. In addition, the battery SOC remains at a value around 40% and the stored hot water is kept at a temperature of 55 °C, compared to the June week of mode OP1 shown in Fig. 6, where the battery SOC and the stored hot water temperature had a value of 90% and 75 °C respectively.

In this scenario, the solar system coupled with the batteries and the fuel cell is able to supply the power demand during the day, except for the months of December to March, when batteries have to be charged from the grid during the night. The total amount of power extracted from the grid is 318 kWh (Table 1). That way, the annual power bill rises to 313 €/year. Besides, from May to September, a total of 746 kWh can be sold to the grid, generating 38 €/year. In this case, the facility cannot be amortized in the 25-year period considered due to the high cost of the initial inversion and posterior substitution of the components (Fig. 10), which is much higher than the money savings achieved by this operation mode. Besides, there is almost no difference between selling or not selling the output energy, as the amount of money paid for it is negligible compared to the value of cash flow. These results are in line with those found by Eriksson and Gray [30] for a household microgrid. They reported that regardless of the size of the equipment, a system with hydrogen technologies would not be economically attractive.

For the development of the simulations of Mode OP3, after proving the little viability, from the economic point of view, of the inclusion of hydrogen as an energy vector for microgrids in regular homes, it has been decided to use the same microgrid as in the first case. Therefore, these simulations aim to assess whether a more sophisticated operation mode, based on the optimization of an economic objective function, would mean savings and a faster return on investment. An example of the results obtained with this operation mode is shown in Fig. 11, for a one-day simulation, and in Fig. 12, for a week, both in August. In these

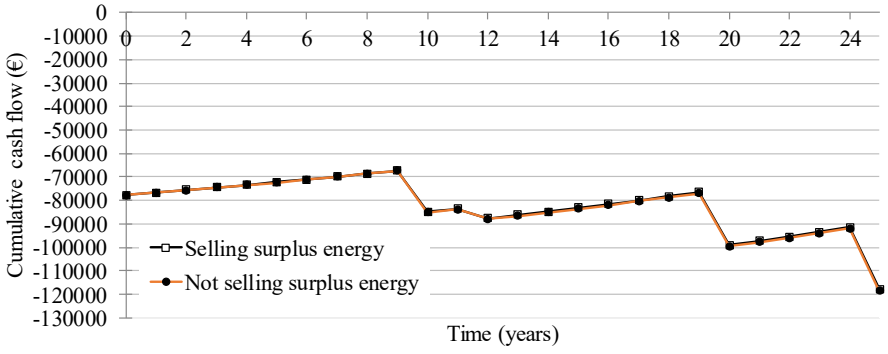

Fig. 10. Cumulative cash flow over the 25-year period.S.

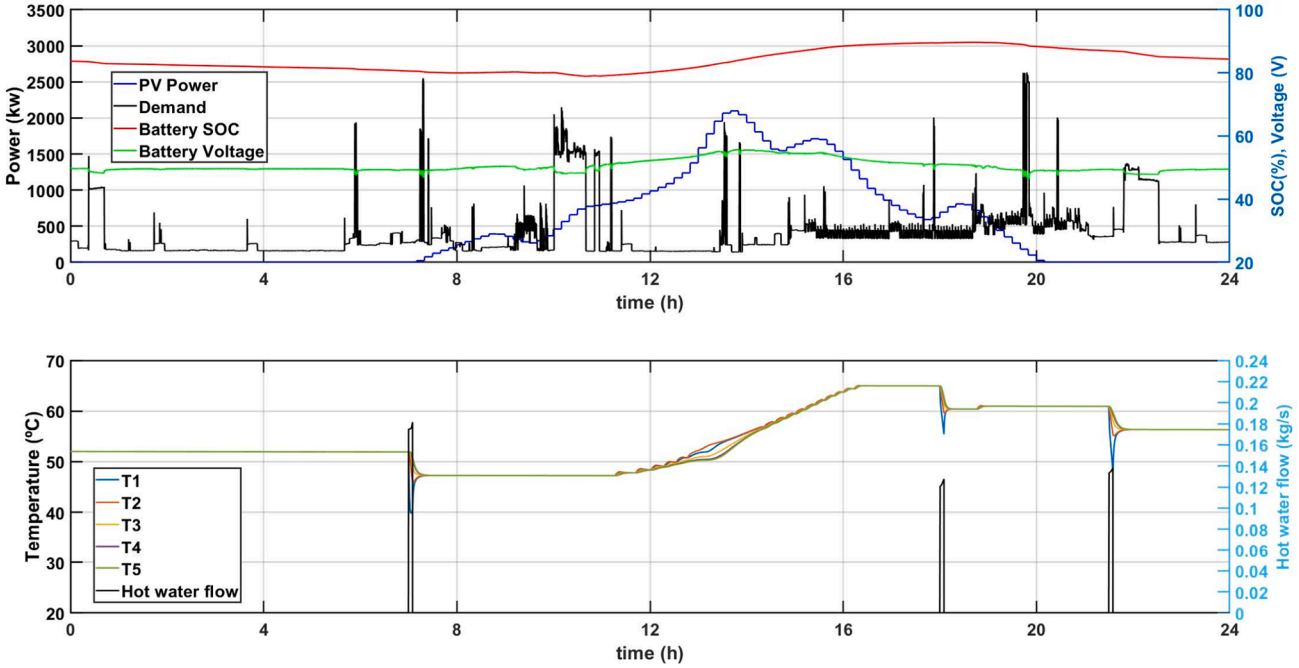

Fig. 11. Simulation result for an August day in Mode OP3 (August 3).

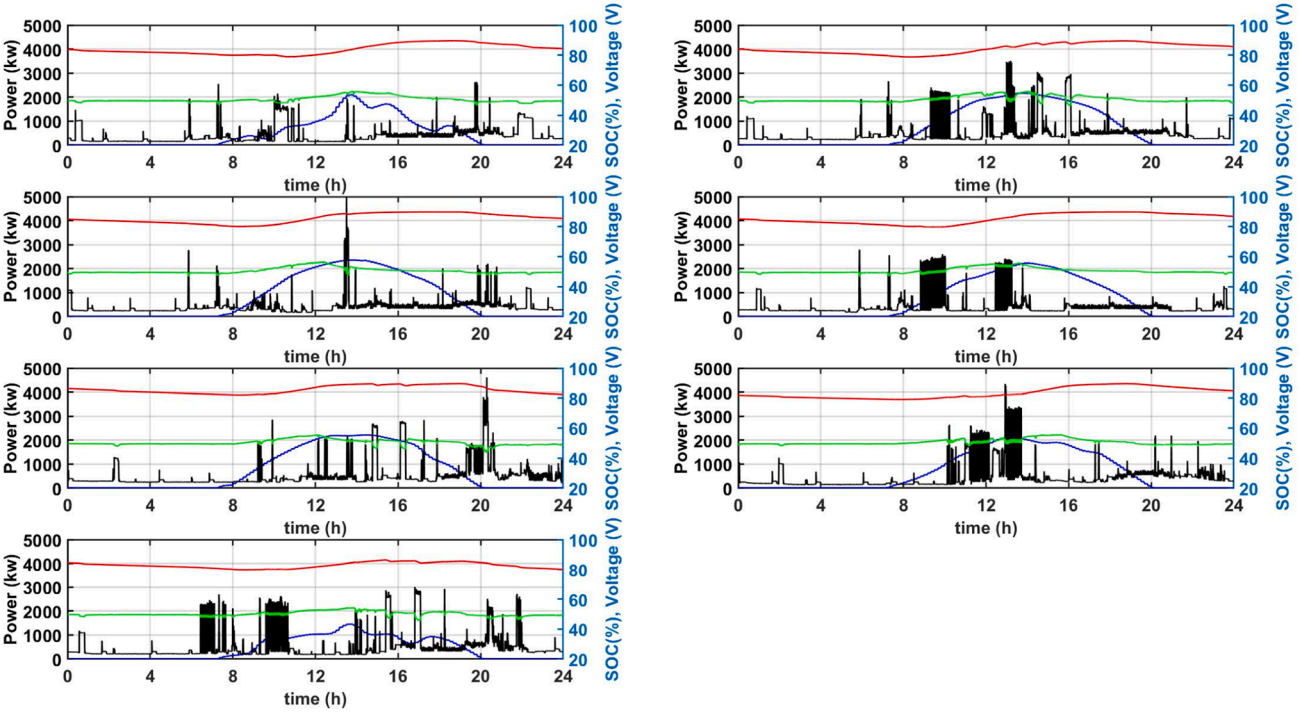

Fig. 12. Simulation of a week in August with the optimal control method. Demand profiles (black), power generated by the photovoltaic field (blue), voltage (green), and state of charge (red) of the batteries.

figures, it can be seen that the changes of the batteries' SOC are smoother than in the previous cases considered, especially in the summer month, where the sale of energy is done in such a way that the state of charge of the batteries is only slightly altered. These smoother changes in the SOC of the batteries result in an extension of their life period.

In this case, the economic results (Fig. 13) do not vary much with respect to the self-regulation mode OP1 (Table 1), since the investment is equal and a more sophisticated control of energy management, at this level of scale, translates into a gain of 44 € per year for the sale of surpluses and better battery management (Table 2), which means extending their useful life by about three years. However, these improvements barely represent a profit of about 240 € at the end of the period considered, which means a 1.75% of economic gain compared to mode OP1.

It is interesting to highlight the use of batteries that each mode of

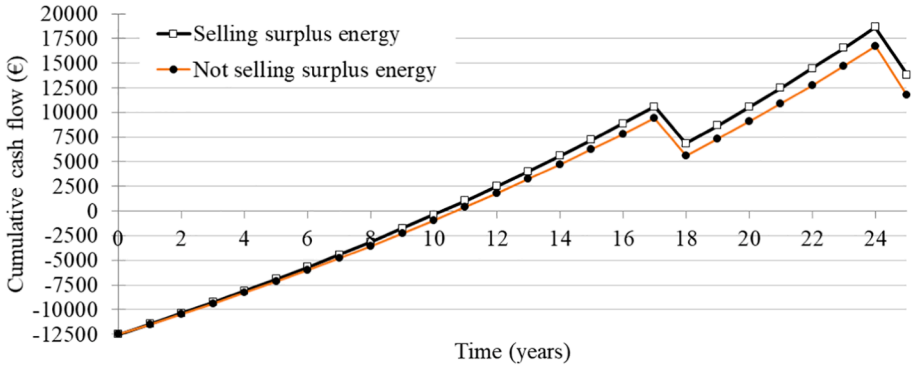

Fig. 13. Cumulative cash flow for scenarios with and without sale of excess energy to the grid in the optimal control case.

Table 2
Comparison of the number of cycles per month and average depth of discharge of the cycles for lead acid batteries with the different simulated modes.

	Number of cycles			Average discharge depth (%)		
	OM1	OM2	OM3	OM1	OM2	OM3
January	35	35	29	12.87	12.87	10.97
February	36	36	28	11.61	11.61	11.48
March	32	24	29	12.65	16.86	9.33
April	25	22	24	12.67	15.45	14.12
May	31	28	44	11.63	11.81	6.53
June	32	28	44	11.49	14.17	6.59
July	28	24	40	12.45	11.60	6.03
August	32	28	48	10.63	11.49	6.19
September	28	28	48	12.17	12.16	6.49
October	28	28	40	12.39	12.38	7.89
November	28	28	30	13.23	13.81	11.82
December	28	28	28	12.28	13.52	11.34
Total/Average	363	337	432	12.17	13.14	9.06

operation makes, since, as expected, the first mode of operation, which is the one that makes the greatest use of batteries, performs a total of 363 charging cycles and discharge with an average depth of discharge of 12.28% (see Table 2), resulting in the shortest useful life of the three modes. The second mode performs a total of 337 cycles with an average depth of discharge of 13.4%, resulting in the longest useful life of the three, which makes sense since, by having hydrogen as a source of electrical energy, it makes less use of batteries. Finally, the third mode of operation performs 432 cycles with an average depth of discharge of 9.06%, which makes the useful life of the batteries between the first and second modes. However, this lengthening of the useful life of batteries results in small economic savings, which may not be enough to justify the use of a more complex control system than that of the first mode of operation.

The simulation results analyzed in this section reveal three key aspects that, in the authors opinion, determine which operation mode is the best suitable for the installation of a microgrid for a residential house:

- For all the operation modes, the isolation from the grid is not economically viable due to the size of the battery system that would be required to do so.
- The use of hydrogen technology for residential houses is clearly not economically viable and therefore, the mode OP2 is clearly discarded.
- The use of an optimal controller instead of a self-regulatory one results in an improvement of 1.75% in the profit at the end of the period. This improvement may be worth it in a large-scale system, but in the case of the residential house studied, it means only around 240 €.

Considering these three key aspects, it seems clear that for the case study, the mode OP1 is the best suitable solution to be implemented.

4. Conclusions

This study shows that the use of microgrids for a single-family home is a technically viable solution, not only in terms of energy demand, but also in terms of power demand which is not study in any other literature to the best of our knowledge. For this scale, the use of hydrogen technologies is technically possible, but economically unfeasible, because of the high investment costs of the necessary equipment.

With the chosen configuration of solar energy and battery storage, the three-inhabitant house still depends on the main electric grid to supply a part of its yearly power-heat demand but for a short and punctual period of time. Furthermore, to be isolated from the main grid, the electric storage system should be increased to store 328 kWh from the 782 kWh energy surplus, instead of being purchased from the grid, making the project inviable not only from a space point of view but also economically. In the case where hydrogen is considered as an energy storage system, a combination of a larger amount of metal hydride bottles or batteries should be considered, making the installation prize even more expensive.

Of the three operation modes considered, the third one, which makes use of an optimization algorithm, manages better the energy use, increasing battery life-spam and economic benefit. However, this increase of 1.75% in the profit of the 25-year period studied may not be enough for a small-scale system to justify the use of a more complex control strategy.

The main barriers for costumers to integrate this kind of installation in existing buildings are the installation cost, the lack of tools the average potential costumer has in order to take informed decisions, and the complexity to install it in existing buildings. This study aims to provide a tool that allows the general public to make decisions supported by experimental data and bring them closer facilitating the penetration of renewable energy in their homes.

CRediT authorship contribution statement

Sergio J. Navas: Conceptualization, Methodology, Software, Validation, Investigation, Writing – original draft, Supervision, Project administration. **G.M. Cabello González:** Methodology, Validation, Formal analysis, Data curation, Visualization, Writing – original draft. **F. J. Pino:** Writing – review & editing, Supervision, Funding acquisition.

Declaration of Competing Interest

The authors declare that they have no known competing financial interests or personal relationships that could have appeared to influence the work reported in this paper.

Acknowledgement

This work has been carried out in the framework of the project "HyBuildings: Diseño, dimensionado y control de micro-redes híbridas térmico-eléctricas basadas en hidrógeno y energías renovables para aplicación en el sector de la edificación" (PY18-RE-0028) funded by Consejería de Conocimiento, Investigación y Universidad of the Junta de Andalucía (Spain). The authors thank the INGEPER research group of the Public University of Navarre, for the power demand data facilitated that has been used in this paper.

References

[1] Shoeb MA, Shafiullah GM. Renewable Energy Integrated Islanded Microgrid for Sustainable Irrigation. A Bangladesh Perspective. Energies 2018;11(5):1283.
[2] Ali I, Shafiullah GM, Urmee T. A preliminary feasibility of roof-mounted solar PV systems in the Maldives. Renew Sustain Energy Rev 2018;83:18–32. https://doi.org/10.1016/j.rser.2017.10.019.
[3] Wirtz C. Energy, Transport and Environment Statistics. 2019.
[4] Hong T, Lee M, Koo C, Jeong K, Kim J. Development of a method for estimating the rooftop solar photovoltaic (PV) potential by analyzing the available rooftop area using Hillshade analysis. Appl Energy 2017;194:320–32. https://doi.org/10.1016/j.apenergy.2016.07.001.
[5] Bódis K, Kougias I, Jäger-Waldau A, Taylor N, Szabó S. A high-resolution geospatial assessment of the rooftop solar photovoltaic potential in the European Union. Renew Sustain Energy Rev 2019;114:109309. https://doi.org/10.1016/j.rser.2019.109309.
[6] Gassar AAA, Cha SH. Review of geographic information systems-based rooftop solar photovoltaic potential estimation approaches at urban scales. Appl Energy 2021;291:116817. https://doi.org/10.1016/j.apenergy.2021.116817.
[7] Walch A, Castello R, Mohajeri N, Scartezzini J-L. Big data mining for the estimation of hourly rooftop photovoltaic potential and its uncertainty. Appl Energy 2020;262:114404. https://doi.org/10.1016/j.apenergy.2019.114404.
[8] Abbasi AR, Seifi AR. Unified electrical and thermal energy expansion planning with considering network reconfiguration. IET Generat Transmission Distribution 2015;9(6):592–601.
[9] Vasebi A, Fesanghary M, Bathaee SMT. Combined heat and power economic dispatch by harmony search algorithm. Int J Electr Power Energy Syst 2007;29:713–9. https://doi.org/10.1016/J.IJEPES.2007.06.006.
[10] Akikur RK, Saidur R, Ping HW, Ullah KR. Comparative study of stand-alone and hybrid solar energy systems suitable for off-grid rural electrification: a review. Renew Sustain Energy Rev 2013;27:738–52. https://doi.org/10.1016/j.rser.2013.06.043.
[11] Karami H, Sanjari MJ, Hosseinian SH, Gharehpetian GB. An optimal dispatch algorithm for managing residential distributed energy resources. IEEE Trans Smart Grid 2014;5:2360–7. https://doi.org/10.1109/TSG.2014.2325912.
[12] Elkadeem MR, Wang S, Sharshir SW, Atia EG. Feasibility analysis and techno-economic design of grid-isolated hybrid renewable energy system for electrification of agriculture and irrigation area: a case study in Dongola. Sudan Energy Convers Manag 2019;196:1453–78. https://doi.org/10.1016/j.enconman.2019.06.085.
[13] Pearce JM. Expanding photovoltaic penetration with residential distributed generation from hybrid solar photovoltaic and combined heat and power systems. Energy 2009;34:1947–54. https://doi.org/10.1016/j.energy.2009.08.012.
[14] Manoj Kumar N, Chopra SS, Chand AA, Elavarasan RM, Shafiullah GM. Hybrid renewable energy microgrid for a residential community: a techno-economic and environmental perspective in the context of the SDG7. Sustainability 2020;12:1–30. https://doi.org/10.3390/SU12103944.
[15] Ranjan Pradhan S, Pragatika Bhuyan P, Sahoo SK, Satya Prasad GRKD. Design of standalone hybrid biomass & PV system of an off-grid house in a remote area. J Eng Res Appl 2013;3:433–7.
[16] Murty VVVSN, Kumar A. Optimal energy management and techno-economic analysis in microgrid with hybrid renewable energy sources. J Mod Power Syst Clean Energy 2020;8:929–40. https://doi.org/10.35833/MPCE.2020.000273.
[17] Mohammadi M, Ghasempour R, Razi Astaraei F, Ahmadi E, Aligholian A, Toopshekan A. Optimal planning of renewable energy resource for a residential house considering economic and reliability criteria. Int J Electr Power Energy Syst 2018;96:261–73. https://doi.org/10.1016/j.ijepes.2017.10.017.
[18] Pranesh V, Velraj R, Christopher S, Kumaresan V. A 50 year review of basic and applied research in compound parabolic concentrating solar thermal collector for domestic and industrial applications. Sol Energy 2019;187:293–340. https://doi.org/10.1016/j.solener.2019.04.056.
[19] Košičan J, Pardo MÁ, Vilčeková S. A multicriteria methodology to select the best installation of solar thermal power in a family house. Energies 2020;13(5):1047.
[20] Zhou X, Tian S, An J, Yan D, Zhang L, Yang J. Modeling occupant behavior's influence on the energy efficiency of solar domestic hot water systems. Appl Energy 2022;309:118503. https://doi.org/10.1016/j.apenergy.2021.118503.
[21] Lamnatou C, Chemisana D. Solar thermal systems for sustainable buildings and climate change mitigation: recycling, storage and avoided environmental impacts based on different electricity mixes. Sol Energy 2022;231:209–27. https://doi.org/10.1016/j.solener.2021.11.022.
[22] Herrando M, Ramos A, Freeman J, Zabalza I, Markides CN. Technoeconomic modelling and optimisation of solar combined heat and power systems based on flat-box PVT collectors for domestic applications. Energy Convers Manag 2018;175:67–85. https://doi.org/10.1016/j.enconman.2018.07.045.
[23] Pardo García N, Zubi G, Pasaoglu G, Dufo-López R. Photovoltaic thermal hybrid solar collector and district heating configurations for a Central European multi-family house. Energy Convers Manag 2017;148:915–24. https://doi.org/10.1016/j.enconman.2017.05.065.
[24] Vassiliades C, Barone G, Buonomano A, Forzano C, Giuzio GF, Palombo A. Assessment of an innovative plug and play PV/T system integrated in a prefabricated house unit: active and passive behaviour and life cycle cost analysis. Renew Energy 2022;186:845–63. https://doi.org/10.1016/j.renene.2021.12.140.
[25] Peláez-Peláez S, Colmenar-Santos A, Pérez-Molina C, Rosales A-E, Rosales-Asensio E. Techno-economic analysis of a heat and power combination system based on hybrid photovoltaic-fuel cell systems using hydrogen as an energy vector. Energy 2021;224:120110.
[26] Natural Resources Canada. Seizing the Opportunities for Hydrogen. 2020.
[27] Duggal I, Venkatesh B. Short-term scheduling of thermal generators and battery storage with depth of discharge-based cost model. IEEE Trans Power Syst 2015;30:2110–8. https://doi.org/10.1109/TPWRS.2014.2352333.
[28] Australian Government Chief Scientist. Hydrogen for Australia's future 2018:59.
[29] Nguyen HQ, Shabani B. Metal hydride thermal management using phase change material in the context of a standalone solar-hydrogen system. Energy Convers Manag 2020;224:113352. https://doi.org/10.1016/j.enconman.2020.113352.
[30] Eriksson ELV, Gray EMA. Optimization of renewable hybrid energy systems – A multi-objective approach. Renew Energy 2019;133:971–99. https://doi.org/10.1016/j.renene.2018.10.053.
[31] Gercek C, Reinders A. Smart appliances for efficient integration of solar energy: a Dutch case study of a residential smart grid pilot. Appl Sci 2019;9(3):581.
[32] Gercek C, Schram W, Lampropoulos I, van Sark W, Reinders A. A comparison of households' energy balance in residential smart grid pilots in the Netherlands. Appl Sci 2019;9(15):2993.
[33] Cau G, Cocco D, Petrollese M. Modeling and simulation of an isolated hybrid micro-grid with hydrogen production and storage. Energy Procedia 2014;45:12–21. https://doi.org/10.1016/j.egypro.2014.01.003.
[34] Valverde L, Rosa F, Bordons C, Guerra J. Energy management strategies in hydrogen smart-grids: a laboratory experience. Int J Hydrogen Energy 2016;41:13715–25. https://doi.org/10.1016/j.ijhydene.2016.05.279.
[35] Higuita Cano M, Agbossou K, Kelouwani S, Dubé Y. Experimental evaluation of a power management system for a hybrid renewable energy system with hydrogen production. Renew Energy 2017;113:1086–98. https://doi.org/10.1016/j.renene.2017.06.066.
[36] Liu Y, Yu S, Zhu Y, Wang D, Liu J. Modeling, planning, application and management of energy systems for isolated areas: a review. Renew Sustain Energy Rev 2018;82:460–70. https://doi.org/10.1016/j.rser.2017.09.063.
[37] Valverde L, Rosa F, Bordons C. Design, planning and management of a hydrogen-based microgrid. Ind Informatics, IEEE Trans 2013;9:1398–404. https://doi.org/10.1109/TII.2013.2246576.
[38] Valverde L, Pino FJ, Guerra J, Rosa F. Definition, analysis and experimental investigation of operation modes in hydrogen-renewable-based power plants incorporating hybrid energy storage. Energy Convers Manag 2016;113:290–311. https://doi.org/10.1016/j.enconman.2016.01.036.
[39] Valverde L. Gestión de energía en sistemas con fuentes renovables y almacenamiento de energía basado en hidrógeno mediante control predictivo 2013.
[40] Petrollese M, Valverde L, Cocco D, Cau G, Guerra J. Real-time integration of optimal generation scheduling with MPC for the energy management of a renewable hydrogen-based microgrid. Appl Energy 2016;166:96–106. https://doi.org/10.1016/j.apenergy.2016.01.014.
[41] Velarde P, Valverde L, Maestre JM, Ocampo-Martinez C, Bordons C. On the comparison of stochastic model predictive control strategies applied to a hydrogen-based microgrid. J Power Sources 2017;343:161–73. https://doi.org/10.1016/j.jpowsour.2017.01.015.
[42] Singh A, Baredar P, Gupta B. Techno-economic feasibility analysis of hydrogen fuel cell and solar photovoltaic hybrid renewable energy system for academic research building. Energy Convers Manag 2017;145:398–414. https://doi.org/10.1016/j.enconman.2017.05.014.
[43] Duffie JA, Beckman WA. Solar engineering of thermal processes. 4th ed. Wiley; 2013.
[44] Dufo-López R, Lujano-Rojas JM, Bernal-Agustín JL. Comparison of different lead–acid battery lifetime prediction models for use in simulation of stand-alone photovoltaic systems. Appl Energy 2014;115:242–53. https://doi.org/10.1016/j.apenergy.2013.11.021.
[45] Bayo O, Sanchis P, Pascual JM. Sistema de baterías para reducción de la potencia consumida en viviendas domésticas: análisis y dimensionado óptimo. Univ Pública Navarra 2014:65.